TITLE
ASP Conference Series, Vol. **VOLUME**, **PUBLICATION YEAR**
EDITORS

GHASP. A 3D Survey of Spiral and Irregular Galaxies at $H\alpha$. Comparison between low and high resolution rotation curves of late-type dwarf galaxies.

Philippe AMRAM & Olivia GARRIDO

Observatoire Astronomique Marseille-Provence & Laboratoire d'Astrophysique de Marseille, 2 Place Le Verrier, 13248 Marseille, Cedex 4, France.

Abstract. This survey, once completed, will provide a 3D sample of 200 nearby spiral and irregular galaxies in the $H\alpha$ line, using a Fabry-Perot system. The data cubes obtained for each galaxy allow derivation of lines maps, velocity fields and higher momentum. The goals of this survey are: (1) To constitute a 3D local reference. (2) To constrain the mass distribution. (3) To constrain the kinematics and dynamics of the internal regions. A data base will be built in order to provide the whole data to the community.

The main result presented in this paper is that, for a sample of 19 late-type dwarfs, the *HI* rotation curves corrected for beam-smearing effects do not agree with the high resolution ones obtained with hybrid $H\alpha/HI$ data. The beam smearing correction done on the *HI* data is on average too strong. The rotation curves rise even more slowly when using hybrid $H\alpha/HI$ data than with *HI* data alone.

1. Introduction

An Homogeneous local sample of data cube. Up to now, it does not exist any homogeneous sample of optical data cube of nearby and isolated spirals with a large range of morphological types and luminosities allowing statistical and individual studies. This data base will constitute an unique and homogeneous 3D sample of velocity fields and line profiles to be used as a reference sample for: (1) comparing nearby galaxies in various environment (clusters, groups, pairs) with field galaxies; (2) studying galaxies at different stages of evolution (interactions, mergers, starbursts, ...) and (3) analyzing galaxies presenting anomalous motions (counter rotating populations, non keplerian motions ...) as well as (4) comparing high redshift galaxies for which 3D data will be available soon with the arrival of intermediate spectral resolution instruments on 8-meter class telescope (e.g. GIRAFFE on the VLT).

Mass distribution of spirals and irregulars. N-body simulations of cosmological evolution have now reached a sufficient resolution to predict dark halos density profiles down to the innermost parts of spiral galaxies. Their trend is to show dense cuspy halos, which are not observed in most cases. High-resolution $H\alpha$ velocity fields are complementary to *HI* velocity fields mapping the outer

galactic regions but suffering of beam smearing and of a lack of emission in the inner regions. The GHASP sample is a sub-sample of the WHISP (Westerbork Survey of *HI* Spiral in Galaxies), lead at Groningen and Dwingeloo, in order to map the neutral hydrogen of some 500 galaxies. The mass distribution of the luminous and dark matter deduced from multi-components mass models is strongly constrained by the inner slope of the rotation curves (RCs), only correctly drawn by 2D velocity fields once corrected for non-circular motions. Accurate inner shape RCs should allow disentangling cosmological scenarii (Blais-Ouellette et al. 2001).

Simulations and theoretical interpretation of velocity fields. In central regions of spiral galaxies, the presence of numerous non-axisymmetric structures like bulges (often triaxials), bars (simple, double/nuclear or triple? bars), circum-nuclei annulus, spiral and inner spiral, ... induces strong velocity gradients and non-axisymmetric velocity fields. To understand and reproduce these structures, fine tuning models are to be compared to the high resolution data cube. On the other hand, with self-consistent model, it will not be possible to match each individual velocity field with all details but it is possible to built a grid in the space parameter (mass of the galaxies, morphological type) in testing the good sets of initial parameters.

In paper, section 4, we will mainly focus on the comparison between the RCs and the mass distribution of a sub-sample of late-type dwarf galaxies obtained firstly in the *HI* 21cm-line alone and secondly in combining $H\alpha$ and *HI*. In section 2, we will describe the galaxy sample, the observations and the data reduction procedures. In section 3, we will explain on several examples why one needs a 3D local reference sample as well as for galaxies in different environments (binaries, groups, clusters) in the local universe as for high redshift galaxies. In section 5, we will give some details on the simulations. In section 6, we will conclude, summarize and provide some issues.

2. Galaxy sample, observations and data reductions.

Observations and data reduction. Observations began in 1998, using a scanning Fabry-Perot at the 1.93m telescope at OHP. Similar observations have begun in March 2001, using the same instrumentation at 1.6m telescope of Mont-Mégantic Observatory (Québec). The GHASP instrument is attached at the Cassegrain focus of the 1.93m telescope at OHP. The original f/15 aperture ratio of the telescope is brought to f/3.9 through the focal reducer. Interferential filters (typical FWHM 1.0 to 1.5 nm) enable to select the $H\alpha$ line of ionized hydrogen (656.278 nm). The $H\alpha$ line is scanned by moving the plates of the interferometer, providing a velocity accuracy of some $km\ s^{-1}$ when the signal to noise ratio is sufficient. A Fabry-Perot interferometer with a free spectral range of $\sim$ 380 $km\ s^{-1}$ at $H\alpha$ and a effective finesse of 12 is used, the free spectral range is scanned through 24 channels. The total field of view is 5.8 arcmin square and the pixel size 0.68 arcsec. The detector is an Image Photon Counting System (GaAs IPCS). The GHASP data are reduced with the ADHOCw software. For more detail see Hernandez et al, this meeting; Gach et al., 2002; Garrido et al. 2002; www-obs.cnrs-mrs.fr/interferometrie/GHASP/ghasp.html; www-obs.cnrs-mrs.fr/interferometrie/instrumentation.html#GaAs).

Galaxy sample. A sample of 200 galaxies has been decided to be a good compromise between the necessary amounts of data to obtain a significant sample in *ad equation* with the scientific goals and a reasonable number of observing runs for the data acquisition on the telescope. On average, a complete observation (including calibrations) of a galaxy can be achieved in 2 hours. For an eight-hours of dark time per night, 4 galaxies can be observed per night. At Haute-Provence Observatory (OHP, France), the average atmospheric conditions provide an efficiency rate of 50%. With a rate of two runs of about 10-12 nights per year, 40 galaxy per year could be obtained. Furthermore, the survey should go on for about 5 years. Scientifically, we expect to cover and sample the plane (galaxy mass - galaxy morphological type). For convenient reasons, we use the plane luminosity-morphological type in the ranges $-16 < M_B < -23$ and $1 < T < 10$. Eight galaxies per bin of 1.4 in magnitude $\times$ 2 in morphological type are observed, this leads to a total amount of 200 galaxies ($8{\times}5{\times}5 = 200$). Non-barred galaxy as well barred galaxies are selected in each bin. M_B has been chosen because it is a simple *a priori* observational criteria, nevertheless it is not the best physical indicator of the total mass of a galaxy , M_R, M_I, M_H, are better ones but they are not available for a large range of galaxies. Furthermore, the sample is readjusted once the data have been reduced in order to extract the maximum rotational velocity of the galaxy, which is the best indicator of the total, mass at least within the optical radius. Maximum rotational velocity ranges between 50 and 350 $km\ s^{-1}$.

3. A Local Reference sample.

An homogeneous sample of optical data cubes of nearby and isolated spirals with a large range of morphological types, luminosities and mass will allow statistical and individual studies of kinematics and dynamics of galaxies in various environments in the nearby and in the far universe.

The Nearby Universe. To disentangle the intrinsic kinematics proprieties of galaxies, including the effects of mass, luminosity and morphological type from the effects linked to peculiar environments, a large sample of isolated galaxies is as much necessary as samples of peculiar galaxies. By peculiar environments one generally refers to the presence of nearby galaxies or intergalactic gas, i.e. to high-density environments (like galaxies in pairs, groups, clusters) at different stages of evolution (like interactions, mergers, starbursts) and sometimes presenting anomalous motions (counter rotating populations -star or gas-, non-axisymetric motions and other anomalous features). In the hierarchical scenario, observationally confirmed by the Hubble Deep Fields studies, a consensus is emerging that, at early epochs, all the galaxies-in-formation were strongly interacting, at least to collapse and form the large galaxies observed today. In a certain sense, any form of galaxy interactions observed today could be considered as a nearby laboratory of the earlier universe, especially for small galaxies, relatively metal poor, in dense environments. Blue Compact Galaxies (BCGs), are supposed to be non-evolved galaxies experiencing an acceleration of their evolution (with respect to their star formation history) at present or recent epochs. Except that BCGs are often relatively isolated objects, they could be present relics of earlier epochs. They are characterised by small to intermediate sizes,

low chemical abundances, high-star formation rate (per luminosity), HII-region-like-emission spectra, absolute B-magnitude ranging between -12 and -21, often surrounded by large *HI* clouds. An important issue for a better understanding of these objects is the knowledge of the non-continuous mechanisms triggering the present star formation. Among different hypothesis, cyclic infall of colded gas, galaxy interactions and collapse of proto-clouds are proposed. From a sample of 6 BCGs + 2 star forming galaxies, Östlin & al. (2001), Amram & Östlin (2001), proposed that the star formation is triggering by recent merging of gas rich objects. If the present environment of these objects is relatively poor, it could have been different in a recent past. A more complete sample of about 20 galaxies has been observed and is presently analyzed. Nevertheless, to achieve more conclusive results, careful calibration should be done with similar but isolated galaxies that do not experience star formation burst. Indeed, a massive star formation could induce strong winds affecting the gas dynamics. Galaxies in compact group of galaxies (CGGs) (1) are the galaxies in the more dense environment of the nearby universe (2) experiencing high rate of galaxy-galaxy interactions and sometimes galaxy-intergalactic gas interaction and (3) are probably also progenitor of galaxies in formation (tidal dwarf galaxy candidates in heavily interacting systems) in that way, they mimic the early universe. Nevertheless, they are different from the first galaxies because they are generally large galaxies and are not so different from field galaxies. It is really a challenge to quantify in these galaxies the rate of interaction and merging with respect to the evolution of CGGs. From a sample of 31 groups (for a total of 104 galaxies), see Plana et al in the present proceeding, we are going (1) to classify the groups in different evolutionary stages of the group (merging groups, strongly interacting groups, weakly interacting groups, non-groups and single irregular galaxies); (2) to built the Tully-Fisher (TF) relation CGGs and (3) to search for tidal dwarf galaxy candidates. Here also it is absolutely obvious that the calibration of the TF relation as well as the systematic studies of kinematical perturbations with respect to their dense environment need a reference sample of isolated galaxies obtained and analysed homogeneously with the same techniques. Galaxies in clusters are probably observed at more advanced stages of interactions than field galaxies with respect to *HI* deficiencies, *HI* and $H\alpha$ truncated disks, low star formation rate (by the lack of fuelling gas), associated radio sources (see e.g. Vollmer et al 2000 an example in Virgo and Gavazzi et al. 2001 for an example in Abell 1367). In clusters, an observational kinematical link is probably missing between the relatively weakly disturbed spirals and the large ratio of early type galaxies supposed to be formed from these spirals. For cluster galaxies also, a reference sample of isolated galaxies is dramatically needed to quantify the kinematical perturbations in spiral -if any- and the processes of violent relation leading to the observed high fraction of lenticular and elliptical galaxies. The same type of arguments could be declined for shells in early-type galaxies that are considered among the "bona fide" signature of a past interaction event. Dynamics of warm gas component, present in some shell galaxies combined with stellar populations is used to constrain the accretion/interaction episode (see Rampazzo et al in the same proceeding). Identically, binary galaxy-galaxy interactions, for which the RCs are often non-flat (see Isaura Fuentes-Carrera in the same proceeding) should be interpreted through the frame of a reference sample.

The distant universe. Up to now, few observations using long-slit spectroscopy at relatively low spectral resolution with very large telescopes have revealed the kinematics of distant galaxies. With the arrival of intermediate spectral resolution instruments on 8-meter class telescope (e.g. GIRAFFE on the VLT), in the next years, 3D samples of high redshift galaxies will be studied (see Chemin et al., this proceeding). The comparison with 3D local samples like GHASP will be necessary to disentangle the effects of secular evolution from the effects link to the environment like those described in the previous section.

4. Mass distribution of late-type dwarf galaxies.

Dwarf galaxies are dark matter-dominated galaxies where the stellar population make only a small contribution to the observed RC, sometimes less important than the gaseous contribution. It is therefore straightforward to compare the observed RCs of these galaxies with those derived from numerical cosmological simulations, where the dark matter is the dominant component.

***HI* observations.** A neutral hydrogen analysis of a sample of 60 RCs of late-type dwarf galaxies has been performed by Swaters in his PhD thesis (1999, hereafter refereed as S99). The S99's observations is a part of the WHISP (Westerbork survey of *HI* in SPiral galaxies) led at Westerbork (Netherlands). Began in 1993, WHISP is a survey of the neutral component in spiral and irregular galaxies with the Westerbork Synthesis Radio Telescope (WSRT) at 21cm wavelength. Its aim is to obtain maps of the distribution and velocity structure of *HI* for some 500 galaxies. Such a uniform database will serve as a basis for research in many areas: dark halos, effects of environment on the structure and growth of *HI* disks, galaxy distances. More details can be found on the Web site http://www.astro.rug.nl/∼whisp/. Once computed from the *HI* velocity fields, the S99's RCs were refined iteratively by constructing models of the observations, taking the instrumental resolution into account. With this procedure the author corrected for the effects of beam smearing to a large extent. The beam smearing plays an important role for the steeper RCs, it depends on the inner slope of the RC and on the sampling of the curve (Blais-Ouellette et al,1999; Blais-Ouellette et al, 2001).

Comparison of the $H\alpha$ and *HI* observations The data for nine galaxies over the nineteen galaxies presented in this paper are discussed in Garrido et al. (2002, refereed hereafter as G2002). The others galaxies will be discussed in fore-coming papers. The $H\alpha$ and *HI* RCs have been combined using the following simple rule: when $H\alpha$ data are available they have been used otherwise *HI* data were used. This means that the inner parts of the RCs have been plotted using the $H\alpha$ velocity points while the outer parts with the *HI* data. The $H\alpha$ RCs have been shifted to the inclinations determined for the *HI* data. Best Fit Mass models (BFMs) including three components (luminous disk, dark halo and HI disk) have been performed with both data sets (*HI* alone and hybrid $H\alpha$+*HI*). The method used in this paper to model the mass distribution is described in Carignan & Freeman (1985), slightly generalized in Blais-Ouellette, Amram & Carignan (2001). The luminosity profile, in the R-band (S99), is used to probe the mass dominant stellar component. The luminosity profile is transformed into a mass distribution for the stellar disk (dash lines in Fig. 1

& 2), assuming a constant mass-to-light ratio $(M/L)_R$. For the contribution of the gaseous component, the *HI* radial profile is scaled by 1.33 to account for He (dot-dash line). The difference between the observed RC and the computed contribution to the curve of the luminous (stars & gas) component is thus the contribution of the dark component, which can be represented by a dark spherical halo (dotted lines). BFMs have usually been computed except when the disk vanishes completely, in that case, a MDM is computed as summarized in Table 2.

The format of this paper does not allow us to describe individually all galaxies of the sample. As an example, let us briefly comment the first one. **UGC 2023**: The *HI* RC has a solid body shape reaching almost 80 arcsec (4 kpc). The $H\alpha$ RC has a completely different shape as it is rather flat up to 50 arcsec (2.5 kpc). Nevertheless, there is no $H\alpha$ emission at radius inner than 20 arcsec (1 kpc), furthermore the kinematics of the inner regions is not so well constrained. Using the *HI* data alone, the BFM leads to a weak disk component while the dark halo dominates at all radii! A BFM for the model hybrid $H\alpha/HI$ RC leads to a M/L of 0.4, this low value is unrealistic and is due to the fact that there is no constrain in the inner part of the RC leading to a dominant dark halo. The MDM for the same hybrid RC leads to a value of M/L=4.7 while the dark halo is, in that case, almost negligible. In conclusion, the beam smearing effects are very important for this galaxy even if there is no information in the inner regions of the galaxy.

On figure 2-right, Mass to Luminous ratio of the disk component for the *HI* RCs versus hybrid $HI/H\alpha$ RCs has been plotted. The *HI* RC does not provide the same value for the disk M/L than the hybrid RC. The huge dispersion around the medium line (dash line) means that HI RCs obtained after beam smearing corrections on the *HI* data do not agree with the high resolution RCs. There is no systematic and predictable in the beam smearing correction. Nevertheless, the disk M/L computed from the *HI* RC is greater than the one computed from the hybrid RC for the 2/3 of this sample of 19 galaxies, for the other third of the sample it is the opposite. The beam smearing correction done on the *HI* data is on average too strong. This leads to an over estimation of the disk M/L ratio and by consequence a under estimation of the dark halo component in *HI*. The RCs for late type dwarf galaxies rise even more slowly when using hybrid $H\alpha/HI$ data than with *HI* data alone. The mass of visible matter is then overestimated in *HI*.

5. Simulations Theoretical interpretation of velocity fields.

Parallel to the observations, the velocity fields are modelled, completing the works on the kinematics of the stars (Wozniak & Pfenniger 1997). We plan to perform the models on two levels:
(A) In a global way, one tries to characterize the velocity fields according to the morphological type, mass and environment of the galaxy. The models are generic; the results of models are statistically compared to the observations. The codes are adapted to the environment of studied objects. We use: *(i)* A particle-mesh N-BODY code coupled to an hydrodynamical SPH code (Friedli & Benz 1993, Friedli & al. 1996), adapted to the simulations of isolated discs; *(ii)*

(1)	(2)	(3)	(4)	(5)	(6)	(7)	(8)	(9)	(10)
UGC	NGC	type	M_B	D	i	R_M	$R_HI/H\alpha$	R_M/h	h
2023		Im	-16.4	8	18	2.91	1.43	2.35	1.24
2034		Im	-17	11.9	10	4.41	1.88	3.53	1.25
2455	1156	IB(s)m		5	51	2.9	2.06	3.3	0.88
3851	2366	IB(s)m		1.3	40	2.05	1.94	1.41	1.45
4278		SB(s)dm	-19.8	7.5	84	10.78	0.44	4.67	2.31
4305		Im	-16.4	2.1	45	3.36	2.51	3.43	0.98
4325	2552	SA(s)m	-17.7	6.7	41	4.68	1.5	2.66	1.76
4499		SABdm	-16.2	9.1	50	5.95	1.46	4.38	1.36
4543		Sdm	-17	26	65	15.1	1.29	4.47	3.38
5272		Im	-15.8	6.9	65	2.17	0.93	3.39	0.64
5414	3104	IAB(s)m	-16.4	8.2	45	4.01	0.89	2.73	1.47
5721	3274	SABdm	-17	7.1	61	7.76	3.06	2.54	0.44
5829		Im	-17.1	8.3	34	6.69	1	3.96	1.69
6628		Sm	-17.5	11.3	25	5.75	1.09	2.16	2.66
7323	4242	SAB(s)dm	-18.6	6.9	40	4.99	1.06	2.36	2.11
7971	4707	Sm		6.2	38	2.26	1.44	2.4	0.94
8490	5204	SA(s)m	-17.7	2.6	50	5.68	3.48	8.23	0.69
11557		SAB(s)dm	-18.4	18.5	37	8.07	1.04	2.67	3.02
12060		Ibm	-16	11.9	40	8.75	1.21	5.54	1.58

Description of column contents. (1) and (2) Name of galaxy from the UGC and NGC catalogues. (3) Hubble Morphological Type from Swaters,1999 (S99). (4) M_B magnitude from S99. (5) Distance in Mpc from S99. (6) Inclination of the galaxy in the plane of the sky, in degrees, from S99. (7) Maximum radius reached by the hybrid rotation curve (RC) in kpc, , using distances given in column (5). (8) Ratio of maximum radius reached by the HI RC to the $H\alpha$ RC. (9) Ratio of the maximum radius of the RC to the disk scale. (10) Disk scale length of the optical disk in R-band, in kpc, using distances given in column (5).

(1)	(2)	(3)	(4)	(5)	(6)	(7)	(8)
	HI Alone			Hybrid $HI/H\alpha$			
UGC	M/L	R_0	ρ_0	M/L	R_0	ρ_0	Remarks
2023	0.6	36	12	0.4	0.2	1101	
2034	1.7	9.6	2	1.3	3.3	8	
2455	0.6	210.0	6	0.2	276.0	7	
3851	2.7	1.7	20	0.5	2.3	20	
4278	6.8	5.8	6	3.5	139.0	16	mdm
4305	2.6	3	0	2.8	16	0	
4325	5.8	1.8	32	8	9.7	30	mdm
4499	0.2	1.5	52	1.6	1.9	32	
4543	2.9	0.1	27	0.9	1.4	25	
5272	3.2	8.0	22	3.1	55	26	
5414	3.3	5.8	5	0.2	8	10	mdm
5721	1.5	0.6	350	0.7	0.6	380	mdm
5829	3	9.0	4	0.9	10.4	2.6	
6628	1.6	0.1	191	2.9	0.5	10	mdm
7323	1.2	4,0	17	2.2	88	6	
7971	0.6	3	14	2.7	0.1	0	mdm
8490	3.1	1.1	98	1.6	1.3	80	
11557	0.3	2.5	24	0.2	7	5	mdm
12060	3.4	1.3	47	0.8	2.3	45	

Description of column contents. Best-fit mass models has been computed except when the disk vanishes completely, in that case, a maximum disk model is computed, see Column (8). the dark halo is a pseudo-isothermal spheroid. (1) Name of galaxy from the UGC catalogue. Columns (2), (3) and (4) refer to the HI rotation curves alone. Columns (5), (6) and (7) refer to the hybrid $H\alpha$/HI rotation curves. Columns (2) and (5)refer to the disk M/L; columns (3) and (6) to the halo core radius in kpc; columns (4) and (7) to the halo central density in $10^{-3}\ M\odot\ pc^{-3}$.

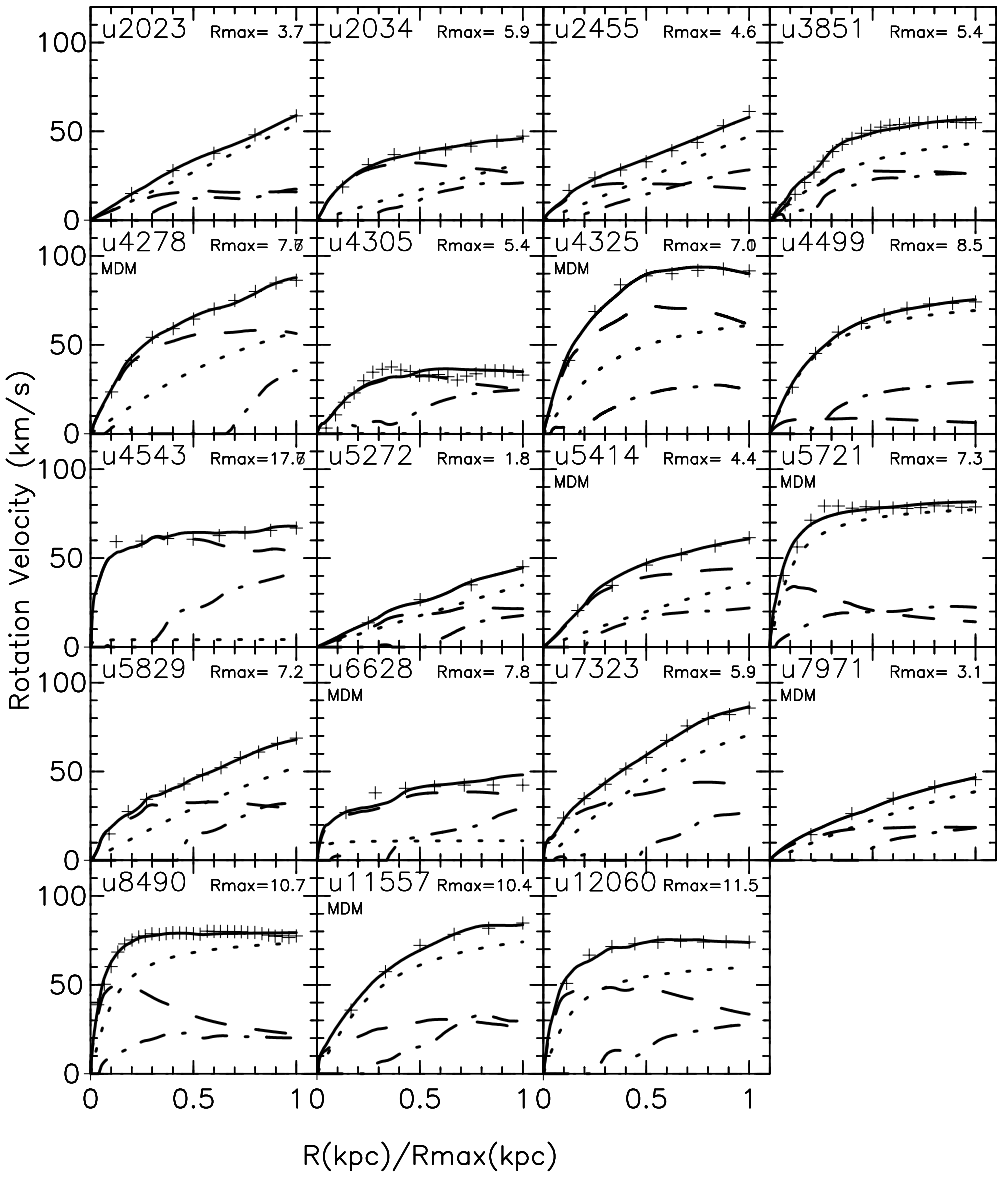

Figure 1. *HI* Rotation curves and mass models for a sample of 19 galaxies. Best fit models are computed except when it leads to a disk equal to zero, it that case a maximum disk model is computed as indicated by (MDM). The x-axis has been scaled to the maximum radius of the rotation curves (Rmax), Rmax are indicated for each galaxy . The symbols "+" are the HI data; the long dashed line is the stellar disk; the dot-dash-dot-dash is the *HI* disk, the dotted line is the pseudo-isothermal dark halo component while the full line is the quadratic sum of the three others components.

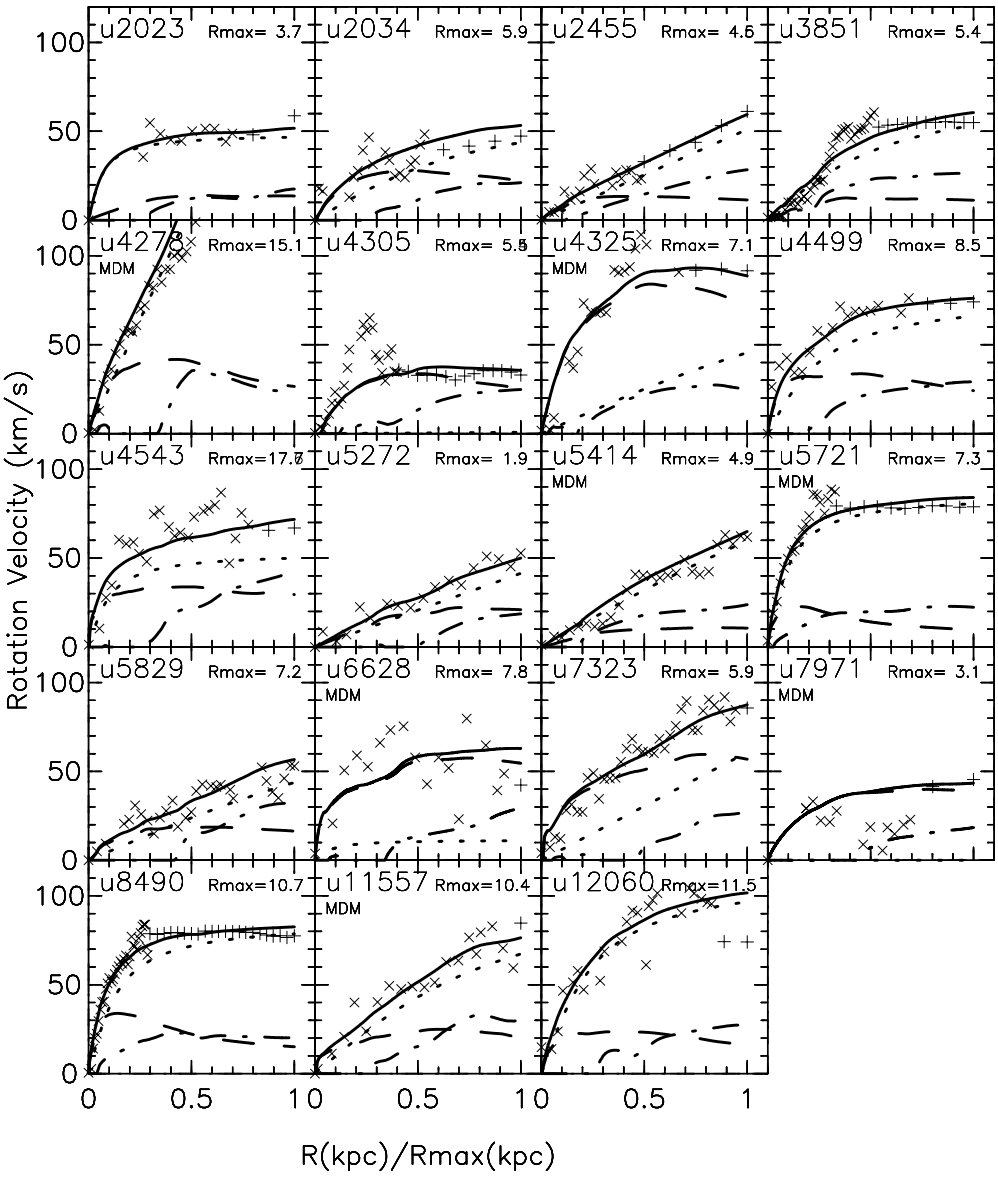

Figure 2. Same as Figure 1 but for the hybrid $HI/H\alpha$ rotation curves. The symbols "$\times$" and "$+$" represent respectively the $H\alpha$ and HI data. Note that the rotation curve of UGC 4278 reaches 240 kms^{-1} and has been truncated by the boundaries fixed for the plot.

A hierarchical N-BODY code coupled to hydrodynamical SPH code (e.g. GADGET N-body, Springel et al, 2001) to simulate galaxies in interaction. Previous studies never focused specifically on kinematical issues. With these simulations, we plan to map and sample the plane (galaxy mass, morphological type) in same ranges than the observations in order to match the models to the observations. The simulations evolve freely from their start point a couple of Gyr ago, the

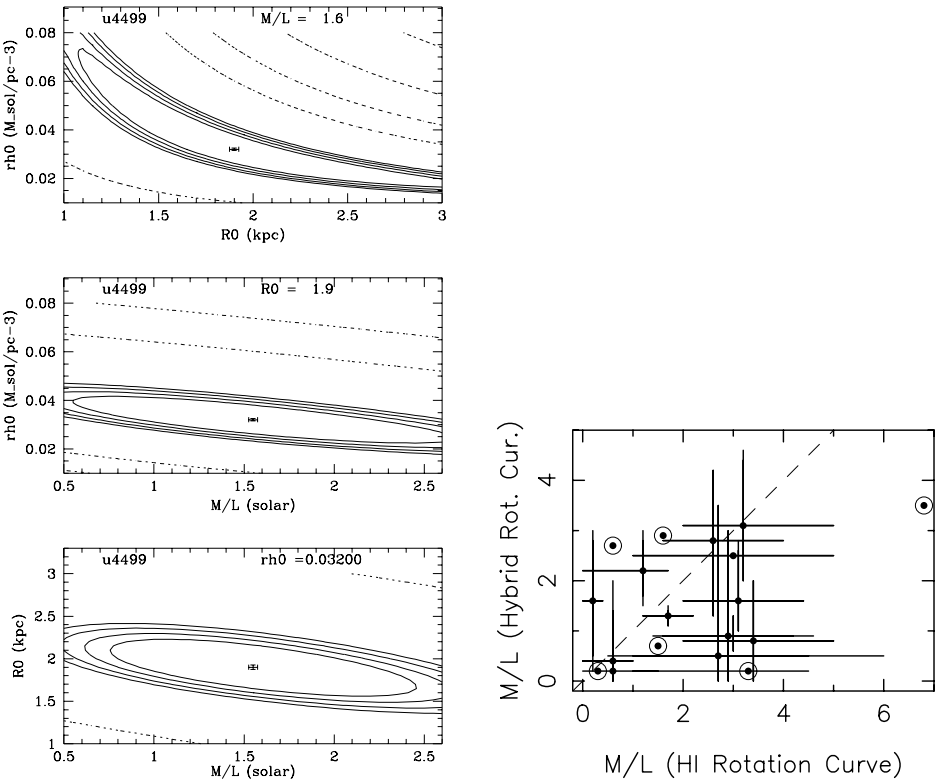

Figure 3. **(left):** χ^2 isocontours for UGC 4499 mass model. The results of the best fit model is plotted here using a pseudo-isothermal sphere. The first line around the cross represents the one-sigma confidence level, the second line, the two-sigma confidence level and so on. Usually, as it is presently the case, it is clear that the M/L parameter is the most difficult to constrain. - **(right):** Mass-to-Luminous ratio of the disk component for the *HI* rotation curves versus hybrid $HI/H\alpha$ rotation curves. The error bars represent the 3-σ levels on the χ^2 confidence contours (like the example plotted on the left-side figure). Only galaxies for which a best-fit model has been computed have an error bar. For the others ones, for which a maximum disk model (MDM) has been computed, the size of the error is represented by the circle around the point. The dashed line represents x=y.

results of the evolution depend only of the given initial conditions (total mass of the galaxy, amount of star and gas, gas to star ratio, disk to halo ratio, ...). **(B)** In an individual way, one tries to model separately each galaxy. The models are here specific. The technique is different: the gravitational potential is determined by photometric observations and the gas flows are simulated by the SPH code in the gravitational potential (e.g. Sempere et al., 1995). Although, the gas is not self-gravitating, the velocity field remains a good approximation in the regions of weak gas density (essentially outside nuclear regions). Finally a theoretical and numerical special attention will be given to the barred galaxies to disentangle the artefacts induced by the presence of the bar in the observational RCs, when the RCs are plotted from the 2D velocity fields without caution with respect to the radial component along the bar.

6. Summary, Conclusions and Issues.

This survey will provide an unique 3D sample of about 200 nearby spiral galaxies in the $H\alpha$ line, using a Fabry-Perot system. The data cubes obtained for each galaxy through their moment analysis allow us to derive crucial kinematical parameters. A data base will be built in order to provide the whole data to the community. The goals of this survey are:

(1) **To constitute a 3D local reference sample of spirals/Irrs.** It has been shown in section 3 that, with respect to the interaction with their high density environments, no conclusive evolutionary panel can be drawn without a solid reference sample for cluster's galaxies, compact group galaxies, binary galaxies, shell galaxies, star forming, ... galaxies as well as for high redshift galaxies.

(2) **To constrain the mass distribution of spirals and Irrs.** The present example of late type dwarf galaxies presented here give a good idea of the impact of higher resolution rotations curves (RCs). The main result of this analysis was to show that the *HI* RCs corrected for beam-smearing effects do not agree with the high resolution RCs. The beam smearing correction done on the *HI* data is on average too strong but could be under-estimated as well as over-estimated. The RCs for late type dwarf galaxies rise even more slowly when using hybrid $H\alpha/HI$ data than with *HI* data alone. With the help of the GHASP survey we will explore all the regions in terms of galaxy mass, surface brightness and morphological types. Other shapes for the dark haloes will be tested with the aim to match the dark haloes computed in N-body simulations in a cosmic evolution frame (Kravtsov et al, 1996, Navarro et al, 1996, Burkert 1995, Burkert & Silk 1997, Zhao, 1996). The resolution reached in those simulations allows to predict the inner part of halo density profiles. These profiles could be directly compared to the ones deduced from modelling RCs obtained in combining the high spatial resolution of $H\alpha$ RCs and the extend of *HI* RCs. This will be done in a fore coming paper.

(3) **To constrain the kinematics and dynamics of the internal regions.** Parallel to the observations, modelled of the gaseous velocity fields are performed, completing the works on the kinematics of the stars. Simulations and theoretical interpretation of the gaseous velocity fields in inner regions of spiral needs an homogeneous data base. For that purpose, on one hand, generic

models provide velocity fields characterized by morphological type, mass and environment of the galaxy (hierarchical N-BODY code coupled to hydrodynamical SPH code); on the other hand, a specific model characterizes each galaxy separately; the gravitational potential is determined by photometric observations and the gas flows are simulated by the SPH code in the gravitational potential.

References

Amram P. & Östlin G., the Messenger, 103, (March 2001)

Blais-Ouellette S., Amram P., Carignan C., 2001, AJ, 121, 4, 1952-1964.

Blais-Ouellette S., Carignan C., Amram P. & Côté, S., 1999, AJ, 118, 2123.

Burkert A., 1995, ApJL, 447, L25.

Burkert A. & Silk J., 1997, ApJ, L55.

Carignan C., Freeman K.C., 1985, AJ 294, 494.

Chemin L., Cayatte V., Flores H., Balkowski C. and Amram P. *in the present volume.*

Fuentes-Carrera I., Amram P. & Rosado M. *in the present volume.*

Friedli, D., Wozniak, H., Ricke, M., Martinet, L., Bratschi, P.? 1996, A&AS, 118, 461.

Friedli, D., Benz, W., 1993, A&A, 268, 65.

Hernandez O., Gach J.L., Boulesteix J. & Carignan C. *in the present volume.*

Gach J-L., Hernandez O., Boulesteix J., Amram P., Boissin O., Carignan C., Garrido O., Marcelin M., Öslin G., Rampazzo R. submitted to PASP, 2002.

Garrido O., Marcelin M., Amram P. & Boulesteix J., 2002, submitted to A&A.

Gavazzi G., Marcelin M., Boselli A., Amram P., Vilchez J.M., Iglesias-Paramo J. and Tarenghi M., A&A, 2001, 377, 745.

Kravtsov A.V., Klypin A.A., Bullock J.S. et Primack, J.R. 1998, ApJ 502, 48

Navarro J.F., Frenk C.S., White SDM, 1996, ApJ 462, 563 - 1997, ApJ 490, 493.

Östlin G., Amram P. , Masegosa J., Bergvall N., Boulesteix J. and Márquez I., A&A, 2001, 374, 800.

Plana H., Amram P., Balkowski C. & Mendes de Oliveira C. *in the present volume.*

Rampazzo R., Amram P., Boulesteix J. & al *in the present volume.*

Sempere M.J., Garcia-Burillo S., Combes F., Knapen J.H., 1995 A&A 296, 45.

Springel, V., White, M., Hernquist, L., 2001, ApJ, 549, 681.

Swaters R.,A, 1999, PhD thesis, Rijksuniversiteit Groningen (S99).

Vollmer B., Marcelin M., Amram P., Balkowski C., Cayatte V., Garrido O., A&A , 364, 532-542 (2000).

Wozniak H. & Pfenniger D., 1997, A&A 317, 14.

Zhao H., 1996, MNRAS, 278, 488.

Acknowledgments. We thank all our collaborators on the GHASP project. In particular M. Marcelin[1] for comments on the data; H. Wozniak[1] for providing a simulation of NGC 3893; S. Blais-Ouellette[3] and C. Carignan[3] for making ad-

justments on their mass model programs and also C. Adami[1], C. Balkowski[2], A. Boselli[1], J.Boulesteix[1], V. Cayatte[2] and L. Chemin[2], J.L. Gach[1], O. Hernandez[1], L. Michel-Dansac[1], H. Plana[4], D. Russeil[1] and B. Vollmer[5]. [1]Observatoire Astronomique Marseille-Provence & Laboratoire d'Astrophysique de Marseille; [2]GEPI, Observatoire de Paris-Meudon; [3]Observatoire du Mont Mégantic & Université de Montréal; [4]Observatorio Nacional, Rio de Janeiro and [5]MPIfR Bonn.